

O. GAYER<sup>1,✉</sup>  
Z. SACKS<sup>2</sup>  
E. GALUN<sup>2</sup>  
A. ARIE<sup>1</sup>

# Temperature and wavelength dependent refractive index equations for MgO-doped congruent and stoichiometric LiNbO<sub>3</sub>

<sup>1</sup> Department of Physical Electronics, School of Electrical Engineering, Tel-Aviv University, Tel-Aviv 69978, Israel

<sup>2</sup> Elbit Systems El-Op Electro-Optics Industries Ltd., Rehovot, Israel

Received: 16 December 2007/

Revised version: 21 February 2008

Published online: 11 April 2008 • © Springer-Verlag 2008

**ABSTRACT** We present wavelength- and temperature-dependent refractive index equations for 5% MgO-doped congruent PPLN and for 1% MgO-doped stoichiometric PPLN crystals valid for a wide spectral and temperature range. The dispersion equations were derived from quasi-phase-matched nonlinear interactions with these two crystal compositions in the near and mid-infrared. The results show a good agreement with previously published frequency conversion experiments.

PACS 42.65.Ky; 42.65.Yj; 42.70.Mp

## 1 Introduction

Periodically poled lithium niobate (PPLN) has been used in a wide variety of nonlinear frequency-conversion applications. In order to design the poling period of such devices and predict their spectral and thermal characteristics, the dependence of the refractive index on wavelength and on temperature must be accurately known. The most commonly used interaction is with the highest non-linear susceptibility tensor element  $d_{33}$  ( $= d_{zzz}$ ), in which the behavior of the extra-ordinary refractive index  $n_e(\lambda, T)$  is desired. In some cases though, the ordinary refractive index  $n_o(\lambda, T)$  is also of interest.

The first PPLN crystals to be applied were made of undoped congruent lithium niobate (CLN), for which there is accurate data from the literature [1, 2]. However, congruent LiNbO<sub>3</sub> is subject to photorefractive damage at temperature below 150 °C and suffers from high coercive field that limits the thickness of poling to about 0.5 mm. In order to solve these drawbacks, two improvements were introduced into the crystals: 1) Adding MgO to the crystal with typical 5% molar doping level; 2) Growing stoichiometric or near stoichiometric lithium niobate (SLN).

Although there are several works on the refractive index properties of MgO-doped CLN [3–8], the data obtained so far is not sufficient. In the work of Zelmon et al. [3], Sellmeier equations were introduced for both  $n_e$  and  $n_o$  in

the spectral range of 0.4–4.8 μm for a constant temperature of 21 °C. However, a comparison with other published works [4, 12] showed discrepancies between the  $n_e(\lambda)$  equation and experimental data in the mid-IR. In the work of Paul et al. [4], a Sellmeier equation was introduced for the spectral range of 1.3–5 μm and temperature range of 20–200 °C. A similar equation was introduced by Li et al. [5] for 1.5–1.7 μm, 2.8–3.6 μm spectral range and 30–170 °C. The spectral ranges of these last two equations are not sufficient for some important applications such as frequency doubling of Nd:YAG 1064 nm lasers and of communication lasers around 1550 nm. Other works that are related to MgO-doped CLN produced Sellmeier equations that are even more limited either in the spectral or thermal range [6–8].

There are even fewer works related to MgO-doped SLN: The Sellmeier equations of Nakamura et al. [9] for 0%–4.6% MgO-doped SLN are confined to 440–1050 nm and room temperature only. Schlarb and Betzler [6] introduced a generalized equation for arbitrary Li and MgO concentrations, which is valid for 400–1200 nm and –50–250 °C. No other equations for MgO-doped SLN have been published, to the best of our knowledge.

For these reasons, it is important to obtain wavelength and temperature dependent Sellmeier equations for both MgO-doped CLN and MgO-doped SLN, which will be applicable for a wide spectral and thermal range. In this paper we present the Sellmeier equations that we obtained, by measurements that involve nonlinear interactions with periodically poled crystals of both compositions.

## 2 Experimental methods

In nonlinear interactions that involve frequency conversion, two basic conditions must be satisfied. The first condition is energy conservation of the participating wavelengths:  $\omega_1 = \omega_2 + \omega_3$ . The second condition is phase matching between the propagating waves. In the case of periodically poled crystals with a period of length  $\Lambda$ , collinear quasi-phase-matching for extraordinary polarized waves is achieved by satisfying (1):

$$2\pi \left[ \frac{n_e(\lambda_1, T)}{\lambda_1} - \frac{n_e(\lambda_2, T)}{\lambda_2} - \frac{n_e(\lambda_3, T)}{\lambda_3} - \frac{1}{\Lambda(T)} \right] = \Delta k_{\text{opt}}. \quad (1)$$

✉ Fax: +972-3-6423508, E-mail: gayerofe@post.tau.ac.il

$\Lambda(T)$  is the actual crystal poling period, taking into account thermal expansion.  $\Delta k_{\text{opt}}$  is the optimal phase mismatch, which equals to zero in the case of plane wave, and in general depends on beam focusing [10]. Equation (1) assumes that the non-linear interaction is based on  $d_{33}$  tensor coefficients. The ordinary refractive index can be studied using interactions that rely on  $d_{22}$  coefficient.

In this work, two types of nonlinear interactions were used. The first type is second harmonic generation (SHG), where the fundamental beam  $\lambda_f = \lambda_2 = \lambda_3$  is converted to  $\lambda_{\text{SHG}} = \lambda_1 = 1/2\lambda_f$ . The second one is optical parametric oscillation (OPO), where a pump beam  $\lambda_p = \lambda_1$  is converted into signal and idler wavelengths:  $\lambda_s = \lambda_2, \lambda_i = \lambda_3$ .

In both interactions, determination of the interacting wavelengths and crystal temperature in which quasi-phase-matching is achieved is a source for data on refractive index properties through (1). It is seen from (1), however, that the refractive indices are not determined for each wavelength directly from experimental results, but rather terms that involve indices of two or three different wavelengths, depending on the non-linear process that is applied. Therefore, a numerical method for calculation of the refractive indices is required.

The Sellmeier equation that is assumed for wavelength and temperature dependent refractive index is like the one used by Jundt for undoped CLN [1].

$$n_e^2 = a_1 + b_1 f + \frac{a_2 + b_2 f}{\lambda^2 - (a_3 + b_3 f)^2} + \frac{a_4 + b_4 f}{\lambda^2 - a_5^2} - a_6 \lambda^2. \quad (2)$$

The parameters  $a_3$  and  $a_5$  account for poles in the UV and IR wavelengths, with  $a_2$  and  $a_4$  weights respectively. The  $a_1$  parameter accounts for contributions to the refractive index from plasmons in the far UV, whereas  $a_6$  accounts for phonon absorptions in the far IR. Since the resonance frequencies of these effects are far from the spectral range of interest their terms have simplified expressions [6]. The  $b_i$  parameters account for thermal effects, involving the temperature dependent parameter  $f$  defined as:

$$\begin{aligned} f &= (T - T_0)(T + T_0 + 2 \times 273.16) \\ &= (T - 24.5^\circ\text{C})(T + 570.82). \end{aligned} \quad (3)$$

For each of the two LiNbO<sub>3</sub> compositions under investigation (i.e., MgO-doped CLN and MgO-doped SLN), the  $a_i$  and  $b_i$  parameters for the Sellmeier equation (2) were determined by a procedure of least squares optimization in which the calculated refractive indices were compared with both experimental results and with data from previously published works, in the spectral and temperature ranges where such data was required. In the case of MgO-doped CLN, results from Zelmon et al. [3] for 0.5–4  $\mu\text{m}$  spectral range at room temperature were used for  $n_o$ . In the case of MgO-doped SLN, results from Nakamura et al. [9] for the 440–1050 nm spectral range at room temperature were used for  $n_e$ .

### 3 Experimental setup

Two types of experimental setups were used, for measurements of second harmonic generation and optical parametric oscillation respectively. The first setup is shown in Fig. 1. The optical source for the fundamental beam is a tunable laser, ANDO AQ4321D model, with a spectral range of 1520–1620 nm and up to 6 dBm continuous maximum output power. A 16 dBm EDFA is used to amplify the laser output, reducing the practical wavelength range roughly to 1530–1570 nm. The amplified laser radiation is coupled to a fiberoptic polarization controller, in order to set the light polarization along the extraordinary axis of the crystal, and then collimated into a Gaussian beam and focused to 35  $\mu\text{m}$  waist. The nonlinear crystal is placed in the center of the beam waist, to obtain maximum SHG efficiency, and is staged on a temperature controlled oven with a temperature range of up to 250  $^\circ\text{C}$ . In some measurements near room temperature, the oven was replaced by a thermo-electric cooler, in order to stabilize the crystal's temperature near or below the ambient temperature.

The SHG signal emitted from the crystal is coupled to a silicon photo-diode which is nearly insensitive for fundamental (laser) wavelength, with a dichroic mirror for further separation between fundamental and SHG beams. The radiation is modulated by a chopper and measured by a lock-in amplifier in order to increase sensitivity.

The second type of setup is a singly resonant OPO, pumped by a Q-switched Nd:YLF 1047.5 nm laser (Light-

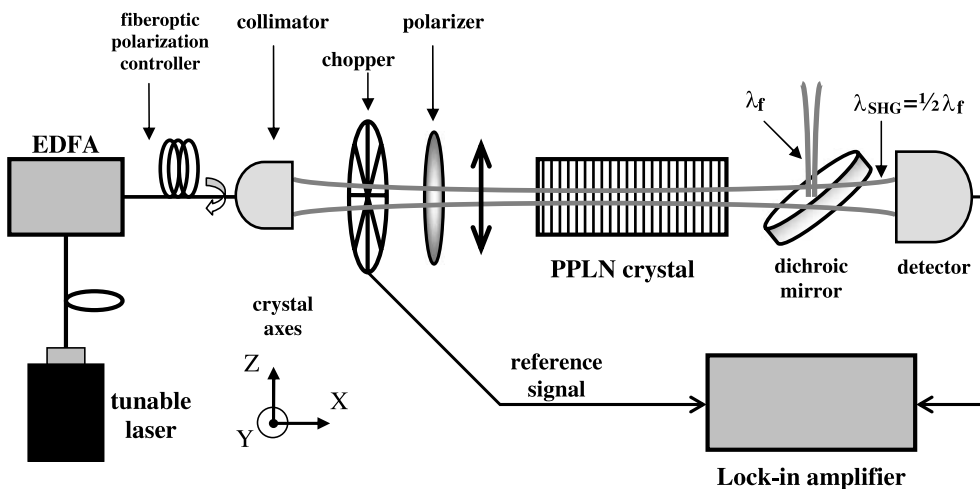


FIGURE 1 Experimental setup for SHG measurements

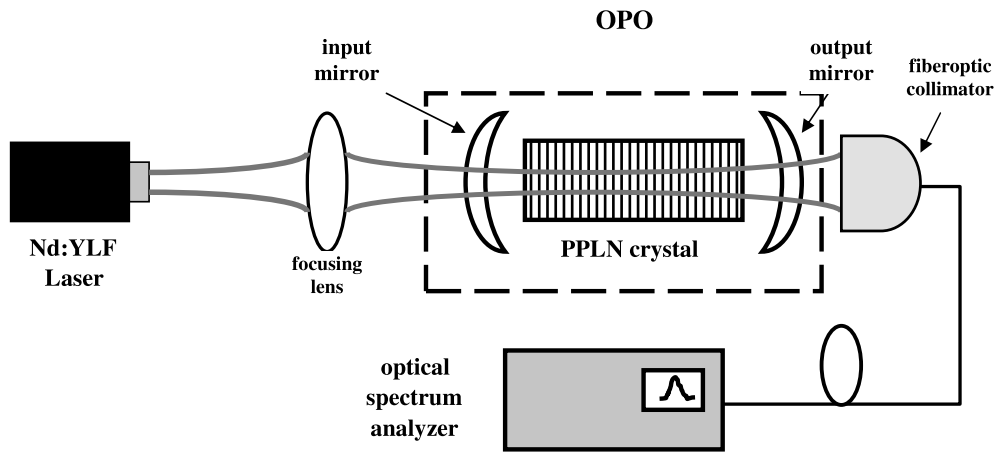


FIGURE 2 Experimental setup for DFG measurements with OPO

wave Electronics model 110), shown in Fig. 2: The laser pump beam is focused to a  $90\ \mu\text{m}$  waist, where the center of the non-linear crystal is placed. The crystal is staged in a controlled temperature oven, with temperature range of up to  $220\ ^\circ\text{C}$ . The input and output coupling mirrors both have  $50\ \text{mm}$  radius of curvature and are placed symmetrically  $20\ \text{mm}$  from crystal surfaces. The signal and idler beams are emitted through the output coupling mirror. The output coupling mirror has approximately  $90\%$  reflectivity at  $1450\ \text{nm}$  and lower reflectivities at higher wavelengths, therefore frequency conversion efficiency is wavelength dependent (though the signal and idler wavelengths depend only on the crystal's period and temperature). The typical characteristic of laser pump pulses are  $8.5\ \text{ns}$  pulse width,  $35\ \mu\text{J}$  energy and  $5\ \text{kHz}$  repetition rate. Idler versus pump efficiencies of up to  $10\%$  were obtained. A spectrum analyzer (ANDO AQ6317B) is used for measurements of signal and idler wavelength. Since the spectrum analyzer is limited to wavelengths up to  $1750\ \text{nm}$ , only signal wavelengths are measured: idler wavelengths are inferred through energy conservation relations. In cases where signal wavelength is above  $1750\ \text{nm}$ , its value is inferred from a secondary weak emission of  $\omega_p + \omega_s$  sum frequency generation that was also detected.

#### 4 Results and discussion

The calculated parameters for the new Sellmeier equations are presented in Table 1. These include  $n_e$  and  $n_o$  for  $5\%$  Mg-doped CLN and  $n_e$  for  $1\%$  Mg-doped SLN. (Note: there are small variations of  $0.1\%$ – $0.2\%$  in Mg doping level between different samples, which are considered negligible.) Figure 3 shows the calculated room temperature dispersion curves  $n(\lambda)$  in the spectral range of  $0.5$ – $4\ \mu\text{m}$ . These include  $n_e$  and  $n_o$  for  $5\%$  Mg-doped CLN and  $n_e$  for  $1\%$  Mg-doped SLN.

##### 4.1 SHG measurements

The crystals that were used for SHG experiments are

MgO-doped CLN:

- 1)  $4.9\%$  MgO-doped crystal, having 6 different evenly spaced gratings between  $18\ \mu\text{m}$  to  $19\ \mu\text{m}$ ,  $10\ \text{mm}$  length, manufactured by Deltronic.

Parameters	5% MgO doped CLN		1% MgO doped SLN
	$n_e$	$n_o$	$n_e$
$a_1$	5.756	5.653	5.078
$a_2$	0.0983	0.1185	0.0964
$a_3$	0.2020	0.2091	0.2065
$a_4$	189.32	89.61	61.16
$a_5$	12.52	10.85	10.55
$a_6$	$1.32 \times 10^{-2}$	$1.97 \times 10^{-2}$	$1.59 \times 10^{-2}$
$b_1$	$2.860 \times 10^{-6}$	$7.941 \times 10^{-7}$	$4.677 \times 10^{-7}$
$b_2$	$4.700 \times 10^{-8}$	$3.134 \times 10^{-8}$	$7.822 \times 10^{-8}$
$b_3$	$6.113 \times 10^{-8}$	$-4.641 \times 10^{-9}$	$-2.653 \times 10^{-8}$
$b_4$	$1.516 \times 10^{-4}$	$-2.188 \times 10^{-6}$	$1.096 \times 10^{-4}$

TABLE 1 Calculated Sellmeier coefficients for  $5\%$  MgO-doped congruent LiNbO<sub>3</sub> (CLN) and  $1\%$  MgO-doped stoichiometric LiNbO<sub>3</sub> (SLN), according to (2), where  $\lambda$  is in microns

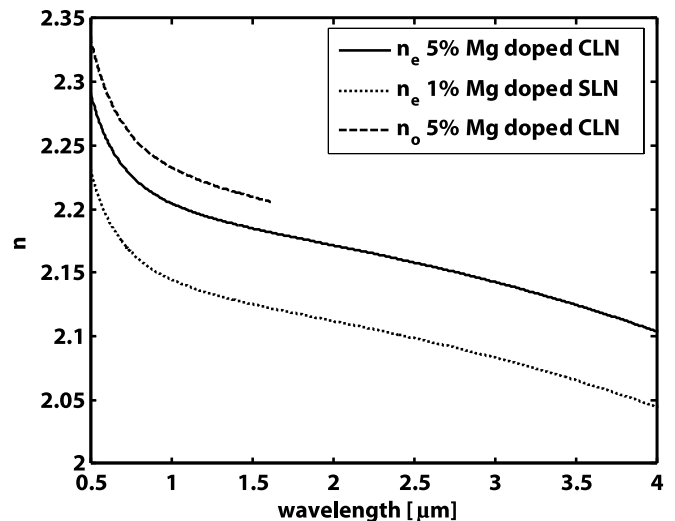


FIGURE 3 Room temperature refractive index curves for  $5\%$  Mg-doped CLN ( $n_e$  and  $n_o$ ), and for  $1\%$  Mg-doped SLN ( $n_e$ ), according to the new Sellmeier parameters given in Table 1

- 2)  $5\%$  MgO-doped crystal  $19.48\ \mu\text{m}$  period,  $10.09\ \text{mm}$  length, manufactured by HC Photonics.

MgO-doped SLN:

- 1.2% MgO-doped crystal,  $19.36\ \mu\text{m}$  period,  $10.16\ \text{mm}$  length, manufactured by HC Photonics.

For each of the above PPLN crystals, SHG measurements were conducted at a wide range of temperatures, from room

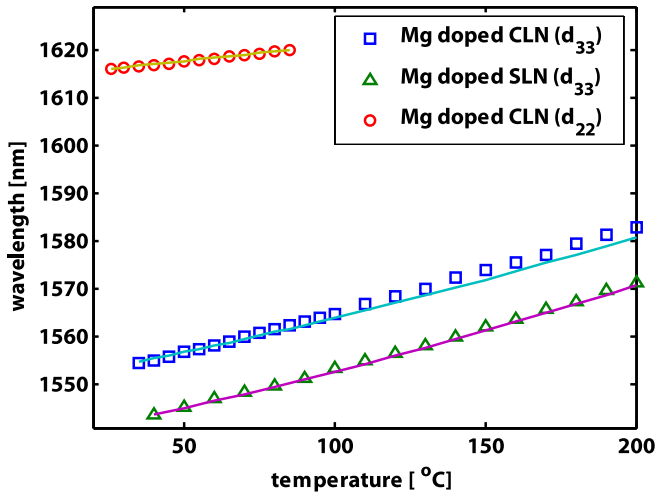


**FIGURE 4** Wavelength vs. temperature curves for phase-matched SHG with: 1) 5% MgO-doped congruent LiNbO<sub>3</sub> (CLN),  $\Lambda = 19.48 \mu\text{m}$  (squares); 2) 1.2% MgO-doped stoichiometric LiNbO<sub>3</sub> (SLN),  $\Lambda = 19.36 \mu\text{m}$  (triangles); 3)  $d_{22}$  interaction with  $n_o$ , for 4.9% MgO-doped CLN,  $\Lambda = 18 \mu\text{m}$  (circles). Results are compared with theoretical curves according to the new Sellmeier equations

temperature to at least 200 °C. For each temperature, the laser wavelength was tuned to a value in which maximum SHG signal was obtained, assuming this wavelength is satisfying phase matching conditions as defined in (1). The dependence of phase-matched wavelength on temperature for 19.48  $\mu\text{m}$  period MgO-doped CLN and 19.36  $\mu\text{m}$  period MgO-doped SLN crystals are shown in Fig. 4. The experimental results in this figure are compared with the theoretical curves according to the Sellmeier parameters calculated in this work (Table 1). In both cases, a good agreement is shown between experimental results and calculated curves. Figure 5 shows the phase matched wavelength for several MgO-doped CLN crystal periods for constant temperature of 21 °C.

The SHG measurements were also applied to determine experimentally the effective non-linearity of the  $d_{33}$  tensor element, using the equation

$$P_{2\omega} = \left[ \frac{Lh2\omega^3 d_{\text{eff}}^2}{\pi n_\omega n_{2\omega} \varepsilon_0 c^4} \right] P_\omega^2. \quad (4)$$

In (4),  $\omega$  and  $2\omega$  are fundamental and SHG frequencies, respectively,  $h$  is the focusing parameter defined by Boyd and Kleinman [10], and  $d_{\text{eff}}$  is the effective non-linear parameter for quasi-phase-matching process. Since the PPLN crystals are uncoated, reflection losses are also taken into account. The measured values for  $d_{\text{eff}}$  are 9.6 pm/V for the MgO-doped CLN sample of Deltronic, 14.2 pm/V for the MgO-doped CLN sample of HC Photonics, and 14.9 pm/V for the MgO-doped SLN sample of HC Photonics. These values are compared with literature value of 15.9 pm/V for 1064 nm SHG process, which according to Miller's rule is equivalent to 15.25 pm/V for 1550 nm SHG. The differences between literature and experimental values may be a result of the quality of the crystals— in the  $d_{\text{eff}}$  calculation a perfect 50% duty cycle poling through the entire crystal is assumed—and inaccuracies in experimental conditions.

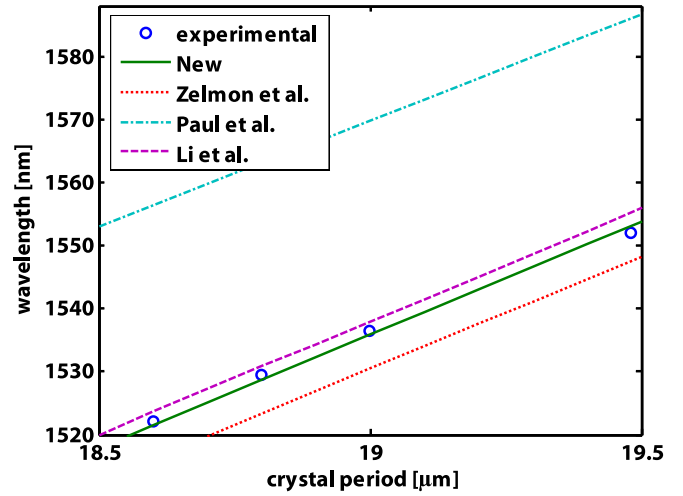


**FIGURE 5** Room temperature phase matched wavelength vs. crystal period for SHG with 5% MgO-doped CLN crystals. Results are compared with theoretical curves according to the new Sellmeier equation and the equations of Zelmon et al. [3], Paul et al. [4] and Li et al. [5]

In a slightly different type of SHG measurements, the spectral range of the experiments was extended, by making use of the fact that these same crystals, which were designed for approximately 1550 nm  $\rightarrow$  775 nm SHG, can also be applied for SHG with 1047.5 nm Nd:YLF laser, satisfying a third order quasi-phase-matching, in which the effective crystal period in (1) is divided by 3. For this purpose, an experimental setup very similar to the one described in Fig. 1 was applied. The only difference was that the tunable laser was replaced with a Nd:YLF laser. Since the laser wavelength cannot be tuned in this case, for each crystal only one temperature was found satisfying (1). Phase matched temperatures of 101.5 °C, 181.1 °C and 166 °C were found for the 19  $\mu\text{m}$ , 19.48  $\mu\text{m}$  5% MgO-doped CLN crystals and for the 19.36  $\mu\text{m}$  1% MgO-doped SLN crystal, respectively. These results were also added to the least squares calculation of the Sellmeier parameters.

Another set of measurements was conducted for the purpose of finding the ordinary axis Sellmeier equation  $n_o(\lambda, T)$ , by using the  $d_{22}(=d_{YY})$  nonlinear tensor element. With this tensor element, both fundamental and SHG waves are Y-polarized; therefore; the conditions for phase matching are determined by the ordinary refractive index  $n_o(\lambda, T)$ . In a previous work it was shown that in PPLN crystals all tensor elements are periodically poled [11], therefore quasi-phase-matching with  $d_{22}$  can be obtained in a similar fashion to  $d_{33}$ . For this purpose, the polarization of the fundamental laser beam in Fig. 1 was rotated to the ordinary axis of the crystal. Also, the EDFA was removed from the setup, since the desired spectral range for SHG is beyond its gain spectral range, though still lies in the range of the ANDO AQ4321D tunable laser. Measurements were confined only to the MgO-doped CLN Deltronic crystal with lowest period available (18  $\mu\text{m}$ ), since higher periods required higher wavelengths beyond the spectral range of this setup. The experimental results of phase-matched wavelength vs. temperature for  $d_{22}$  interaction are also shown in Fig. 4, together with theoretical curves that are based on the new calculated Sellmeier equation for  $n_o(\lambda, T)$ . Good agree-

ment is shown between the experiment and the calculated curve.

#### 4.2 OPO measurements

The following crystals were used for OPO experiments:

MgO-doped CLN:

5% MgO doping, seven different gratings, evenly spaced with 0.5  $\mu\text{m}$  steps between 28.5  $\mu\text{m}$ –31.5  $\mu\text{m}$ , 25 mm length, manufactured by HC Photonics.

MgO-doped SLN:

1) 1.2% MgO doping, 29.08  $\mu\text{m}$  period, 40 mm length, manufactured by HC Photonics.

2) 1% MgO doping, 8 different 28.9–31.35  $\mu\text{m}$  periods, 40 mm length, manufactured by Deltronic.

The OPO signal and idler spectra were measured for all periods in the temperature range of 25–220  $^{\circ}\text{C}$ . The spectra of the MgO-doped CLN and SLN crystals are shown in Figs. 6 and 7 respectively, together with the theoretical spectra based on the calculated Sellmeier equations for these crystal compositions. The combined signal and idler spectra continuously cover all spectral range of 1.4–4  $\mu\text{m}$ . Together with the SHG measurements, the experimental data that were used for calculating the  $n_e(\lambda, T)$  Sellmeier parameters crystals extend from the green visible range into the mid-IR, thus increasing their reliability.

#### 4.3 Comparison with previously published results

The validity of the new Sellmeier equations was compared with all previously published equations and with experimental data that were available from literature.

**4.3.1 MgO-doped CLN.** In the case of 5% MgO-doped CLN crystals, a comparison of different  $n_e(\lambda, T)$  equations with our SHG measurements is shown in Fig. 5: the phase matched wavelengths vs. crystal period are given for a constant temperature of 21  $^{\circ}\text{C}$ , and compared with theoretical curves according to the new equation and the equations of Zelmon et al. [3], Paul et al. [4] and Li et al. [5]. The new equation shows the best agreement with our SHG results. The equation of Li et al. also shows a good agreement with these results, but it failed to agree with our SHG measurements of Nd:YLF 1047.5 nm wavelength (not shown in figure), the temperature deviations exceeding 20  $^{\circ}\text{C}$  (compared to < 2  $^{\circ}\text{C}$  deviations from the new equation).

An example of comparison with experimental data not from the present work is shown in Fig. 8: the room temperature OPO spectrum (signal & idler vs. crystal period) obtained

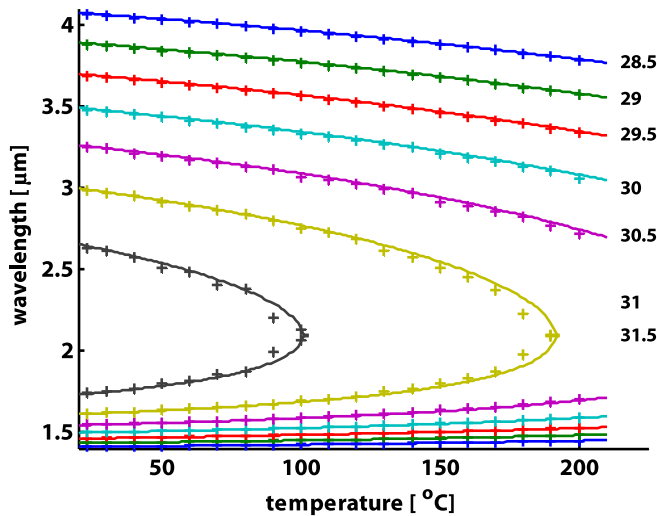


FIGURE 6 Nd:YLF pumped OPO signal and idler spectra of wavelength vs. temperature for 5% MgO-doped congruent LiNbO<sub>3</sub> (CLN),  $\Lambda = 28.5\text{--}31.5$   $\mu\text{m}$  (periods in  $\mu\text{m}$  are listed on the right of each curve). Results are compared with theoretical curves according to the new Sellmeier equation

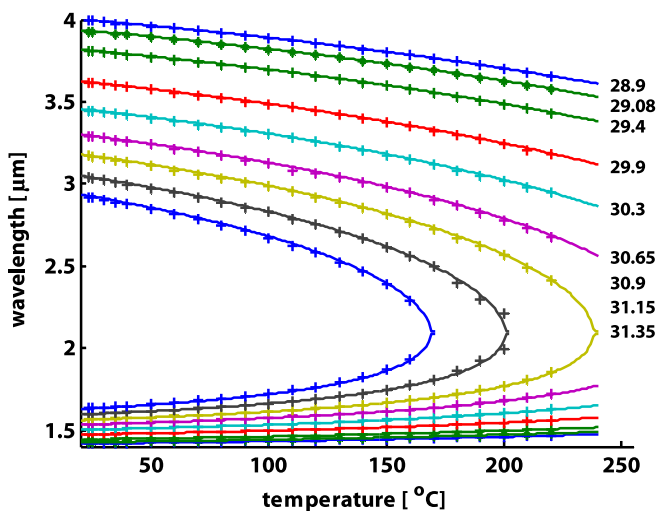


FIGURE 7 Nd:YLF pumped OPO signal and idler spectra of wavelength vs. temperature for 1%–1.2% MgO-doped stoichiometric LiNbO<sub>3</sub> (SLN),  $\Lambda = 28.9\text{--}31.35$   $\mu\text{m}$  (periods in  $\mu\text{m}$  are listed on the right of each curve). Results are compared with theoretical curves according to the new Sellmeier equation

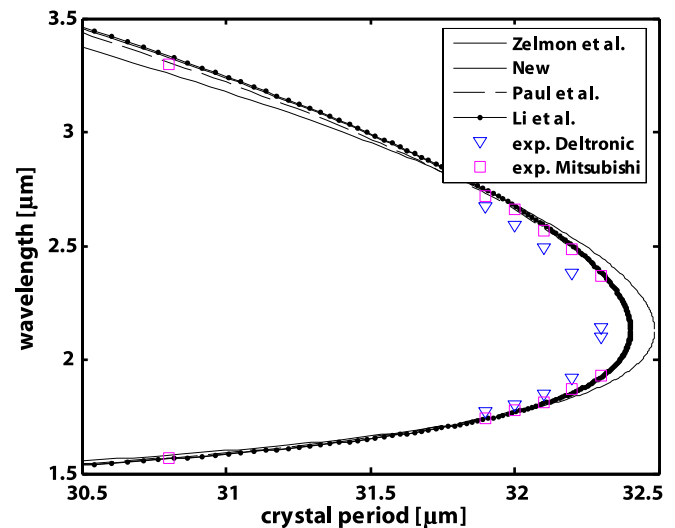


FIGURE 8 Nd:YAG pumped OPO room temperature signal and idler spectra extracted from Yi et al. [12], of wavelength vs. period for 5% MgO-doped CLN crystals from 2 different sources (Deltronic and Mitsubishi). Experimental data is compared with theoretical curves according to the new Sellmeier equation and the equations of Zelmon et al. [3], Paul et al. [4] and Li et al. [5]

from 5% MgO-doped CLN crystals, in the work of Yi et al. [12], is compared with theoretical curves according to the new equation and the equations of Zelmon et al. [3], Paul et al. [4] and Li et al. [5]. All equations show a similar agreement with results, with some deviations near degeneracy, the equation of Zelmon et al. shows the largest deviation.

A quantitative comparison of the new Sellmeier equations with the previously published equations shows that the deviation from Paul et al.'s equation is limited by the following:  $\max|n_{e,\text{new}} - n_{e,\text{Paul}}| < 1.7 \times 10^{-4}$  for the entire 1.05–4  $\mu\text{m}$  spectral range and 20–200  $^{\circ}\text{C}$  temperature range. With Zelmon et al.'s equations (at 21  $^{\circ}\text{C}$ ), the deviations for  $n_e$  are limited by  $\max|n_{e,\text{new}} - n_{e,\text{Zelmon}}| < 3.1 \times 10^{-4}$  for 0.5–3  $\mu\text{m}$ , but exceeding  $2 \times 10^{-3}$  as wavelength approaches 4  $\mu\text{m}$ , for  $n_o$  deviations are limited by:  $\max|n_{o,\text{new}} - n_{o,\text{Zelmon}}| < 2.2 \times 10^{-4}$  for 0.5–5  $\mu\text{m}$ . (Note: these last two comparisons were conducted after switching between Zelmon's  $n_o(\lambda)$  and  $n_e(\lambda)$  equations, since it is believed that in the original paper of Zelmon et al. their parameters were switched by mistake.) A comparison with the  $n_e$  equation of Li et al. [5] showed a nearly constant difference of  $\sim 5 \times 10^{-2}$  between refractive indices for the entire spectral and temperature range. This large difference can be explained by the fact that the equation of Li et al. is based on Jundt's equation for undoped CLN [1], with only one parameter changed. Therefore this equation is valid up to an addition of a constant but is not suitable for applications where absolute values of refractive index are required.

**4.3.2 MgO-doped SLN.** For MgO-doped SLN, Fig. 9 shows the OPO spectra in the work of Huang et al. [15]. A good agreement is shown between experimental data and theoretical curves that are based on our new  $n_e(\lambda, T)$  equation; the small differences can be easily attributed to experimental inaccuracies.

A quantitative comparison between the new Sellmeier equation and the equation of Nakamura et al. [9], in the spectral range of 400–1050 nm (at room temperature), shows

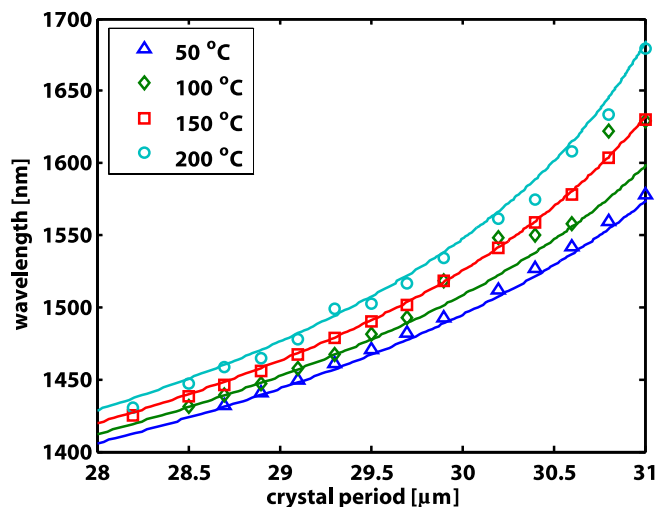


**FIGURE 9** Nd:YAG pumped OPO signal spectra of wavelength vs. period for 1% MgO-doped SLN crystals. Experimental data is from Huang et al. [15], compared with theoretical curves according to new Sellmeier equation

a limit of:  $\max|n_{e,\text{new}} - n_{e,\text{Nakamura}}| < 6.5 \times 10^{-4}$ . A comparison with the equation of Schlarb and Betzler for MgO-doped SLN [6] shows much larger deviations, up to  $1.5 \times 10^{-3}$ . These larger deviations may be explained by the fact that the equation of Schlarb and Betzler is generalized for arbitrary Li and MgO concentrations, and its parameters were not based directly on measurements of MgO-doped SLN samples.

## 5 Summary and conclusions

In this work we present wavelength and temperature-dependent refractive index equations for 5% MgO-doped congruent LiNbO<sub>3</sub> and for 1% MgO-doped stoichiometric LiNbO<sub>3</sub> crystals, which are valid for a wide spectral and temperature range. For 5% MgO-doped congruent LiNbO<sub>3</sub>, equations for both ordinary and extraordinary axes were obtained. The determination of the Sellmeier coefficients is based on measurements of frequency conversion nonlinear interactions and also on other previously published equations available from the literature.

Our new Sellmeier equations are in good agreement with most of the previously published equations, and show the best agreement with both our experimental results and previously published experimental data. The  $n_e(\lambda, T)$  equations for both 5% MgO-doped CLN and 1% MgO-doped SLN are valid for 0.5–4  $\mu\text{m}$  spectral range and 20–200  $^{\circ}\text{C}$  temperature range. Although the 0.5–1.4  $\mu\text{m}$  part of this spectral range is covered only by a small number of measurements, these  $n_e(\lambda, T)$  equations are considered reliable for this part also due to the smooth behavior of the refractive indices. We were not able to test the validity of the  $n_o(\lambda, T)$  equation for MgO-doped CLN in these entire spectral and thermal ranges, therefore it is considered reliable only for wavelengths up to 1620 nm and roughly 20–100  $^{\circ}\text{C}$ . The new Sellmeier equations will be very useful for any future design of nonlinear optical devices that are based on these materials.

## REFERENCES

- 1 D.H. Jundt, *Opt. Lett.* **22**, 1553 (1997)
- 2 L.H. Deng, X.M. Gao, Z.S. Cao, W.D. Chen, Y.Q. Yuan, W.J. Zhang, Z.B. Gong, *Opt. Commun.* **268**, 10 (2006)
- 3 D.E. Zelmon, D.L. Small, D. Jundt, *J. Opt. Soc. Am. B* **14**, 3319 (1997)
- 4 O. Paul, A. Quosig, T. Bauer, M. Nittmann, J. Bartschke, G. Anstett, J.A. L'huillier, *Appl. Phys. B* **86**, 111 (2007)
- 5 H.P. Li, D.Y. Tang, S.P. Ng, J. Kong, *Opt. Laser Technol.* **38**, 192 (2006)
- 6 U. Schlarb, K. Betzler, *Phys. Rev. B* **50**, 751 (1994)
- 7 H.Y. Shen, H. Xu, Z.D. Zeng, W.X. Lin, R.F. Wu, G.F. Xu, *Appl. Opt.* **31**, 6695 (1992)
- 8 S. Lin, Y. Tanaka, S. Takeuchi, T. Suzuki, *IEEE J. Quantum Electron.* **QE-32**, 124 (1996)
- 9 M. Nakamura, S. Higuchi, S. Takekawa, K. Terabe, Y. Furukawa, K. Kitamura, *Japan. J. Appl. Phys.* **41**, L49 (2002)
- 10 G.D. Boyd, D.A. Kleinman, *J. Appl. Opt.* **39**, 3597 (1968)
- 11 A. Ganany, A. Arie, S.M. Saltiel, *Appl. Phys. B* **85**, 97 (2006)
- 12 J. Yi, H. Ishizuki, I. Shoji, T. Taira, S. Kurimura, *J. Korean Phys. Soc.* **47**, 439 (2005)
- 13 Y.L. Chen, J.W. Yuan, C.F. Yan, J.J. Xu, G.Y. Zhang, *Opt. Commun.* **273**, 560 (2007)
- 14 H.C. Guo, S.H. Tang, Z.D. Gao, Y.Q. Qin, S.N. Zhu, Y.Y. Zhu, *J. Appl. Phys.* **101**, 113 112 (2007)
- 15 L. Huang, D. Hui, D.J. Bamford, S.J. Field, I. Mnushkina, L.E. Myers, J.V. Kayser, *Appl. Phys. B* **72**, 301 (2001)